Supporting Information for "Optimal Basis Set for Electron Dynamics in Strong Laser Fields: The case of Molecular Ion H_2^+"

Marie Labeye[1],* Felipe Zapata[2],* Emanuele Coccia[3], Valérie Véniard[4], Julien Toulouse[2], Jérémie Caillat[1], Richard Taïeb[1], and Eleonora Luppi[2†]

[1]*Laboratoire de Chimie Physique Matière et Rayonnement, Sorbonne Université and CNRS, F-75005 Paris, France*

[2]*Laboratoire de Chimie Théorique, Sorbonne Université and CNRS, F-75005 Paris, France*

[3]*Dipartimento di Scienze Chimiche, Università di Padova, 35131 Padova, Italy*

[4]*Laboratoire des Solides Irradiés, École Polytechnique, Université Paris-Saclay, CEA-DSM-IRAMIS, F-91128 Palaisau, France*

*The first two authors contributed equally to the present work.

†Electronic address: eleonora.luppi@upmc.fr

TABLE S1: Exponents and contraction coefficients of the 1D Gaussian basis set. K indicates the optimal Kaufmann functions for the continuum.

Type	ℓ	Exponents	Contraction coefficients
STO-3G	s	0.109818	1.000000
STO-3G	s	0.405771	1.000000
STO-3G	s	2.22766	1.000000
K	s	0.078927	1.000000
K	s	0.031055	1.000000
K	s	0.016685	1.000000
K	s	0.010442	1.000000
STO-3G	p	0.109818	1.000000
STO-3G	p	0.405771	1.000000
STO-3G	p	2.22766	1.000000
K	p	0.101215	1.000000
K	p	0.052969	1.000000
K	p	0.032646	1.000000
K	p	0.022169	1.000000

TABLE S2: Exponents and contraction coefficients of the 3D Gaussian basis set 6-aug-cc-pVTZ+5K. Type indicates the "origin" of the Gaussian functions, aug the diffuse functions, and K the optimal Kaufmann functions for the continuum.

Type	ℓ	Exponents	Contraction coefficients
cc-pVTZ	s	33.870000	0.006068
		5.095000	0.045308
		1.159000	0.202822
cc-pVTZ	s	0.325800	1.000000
cc-pVTZ	s	0.102700	1.000000
aug	s	0.025260	1.000000
aug	s	0.006210	1.000000
aug	s	0.001530	1.000000
aug	s	0.000377	1.000000
aug	s	0.000093	1.000000
aug	s	0.000023	1.000000
K	s	0.245645	1.000000
K	s	0.098496	1.000000
K	s	0.052725	1.000000
K	s	0.032775	1.000000
K	s	0.022327	1.000000
cc-pVTZ	p	1.407000	1.000000
cc-pVTZ	p	0.388000	1.000000
aug	p	0.102000	1.000000
aug	p	0.026800	1.000000
aug	p	0.007040	1.000000
aug	p	0.001849	1.000000
aug	p	0.000487	1.000000
aug	p	0.000128	1.000000
K	p	0.430082	1.000000
K	p	0.169341	1.000000
K	p	0.089894	1.000000
K	p	0.055611	1.000000
K	p	0.037766	1.000000
cc-pVTZ	d	1.057000	1.000000
aug	d	0.247000	1.000000
aug	d	0.057700	1.000000
aug	d	0.013500	1.000000
aug	d	0.003158	1.000000
aug	d	0.000740	1.000000
aug	d	0.000173	1.000000
K	d	0.622557	1.000000
K	d	0.242161	1.000000
K	d	0.127840	1.000000
K	d	0.078835	1.000000
K	d	0.053428	1.000000

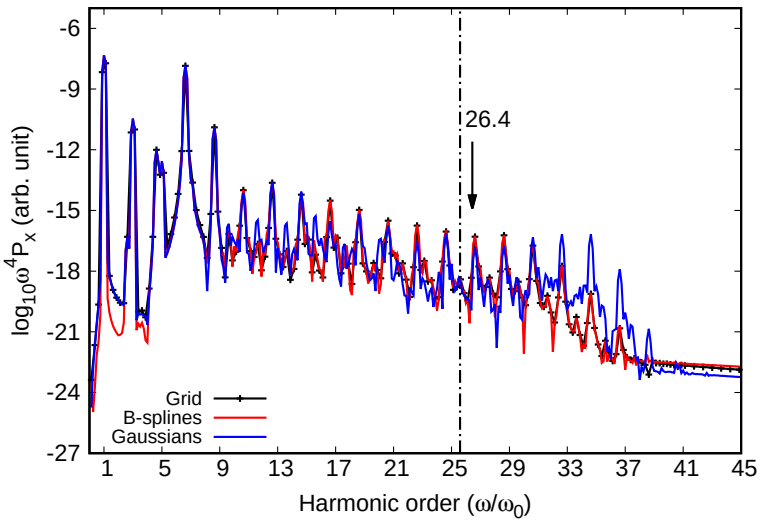

FIG. S1: HHG spectrum from the dipole at $R = 2.0$ au with laser intensity $I = 5 \times 10^{13}$ W/cm^2. The dot-dashed line indicates the energy cutoff $E_{\text{cutoff}} = 25.6\omega_0$. The arrow points the expected position of the two-center interference minimum extracted from the recombination dipole.

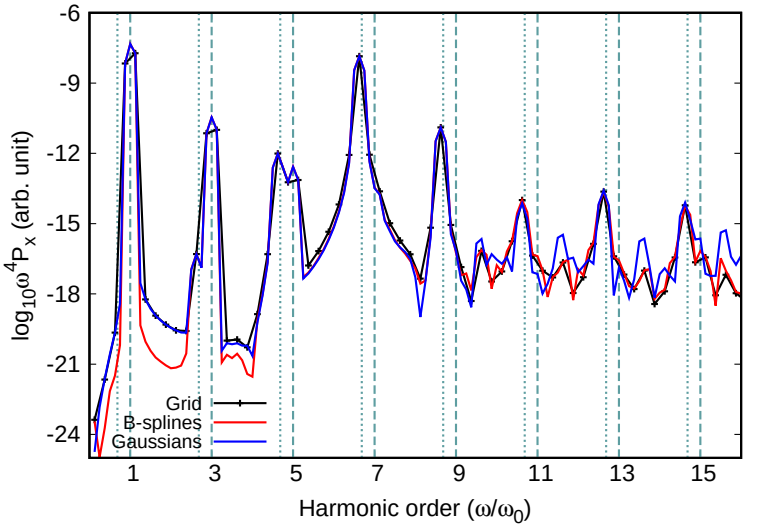

FIG. S2: HHG spectrum from the dipole at $R = 2.0$ au with laser intensity $I = 5 \times 10^{13}$ W/cm^2 up to the 15th harmonic. The dashed line indicates the position of the harmonics while the dotted line indicates the resonances due to the first excited state of H_2^+.

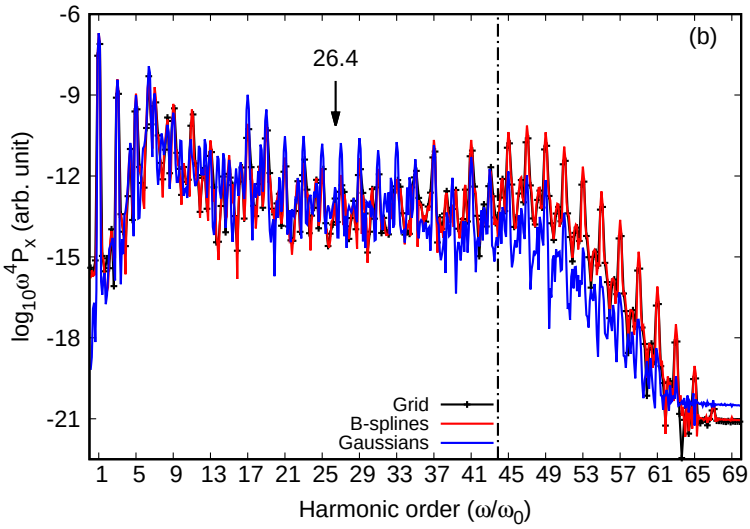

FIG. S3: HHG spectrum from the dipole at $R = 2.0$ au with laser intensity $I = 5 \times 10^{13}$ W/cm^2. The dot-dashed line indicates the energy cutoff $E_{\text{cutoff}} = 25.6\omega_0$. The arrow points the expected position of the two-center interference minimum extracted from the recombination dipole.

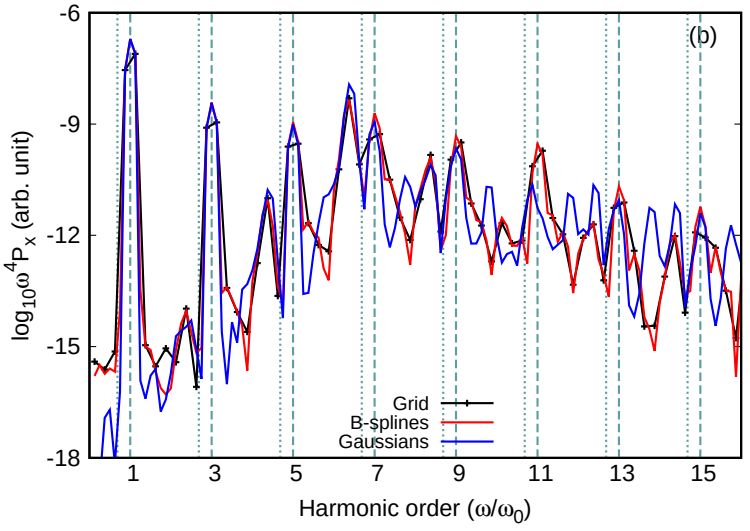

FIG. S4: HHG spectrum from the dipole at $R = 2.0$ au with laser intensity $I = 5 \times 10^{13}$ W/cm^2 up to the 15th harmonic. The dashed line indicates the position of the harmonics while the dotted line indicates the resonances due to the first excited state of H_2^+.

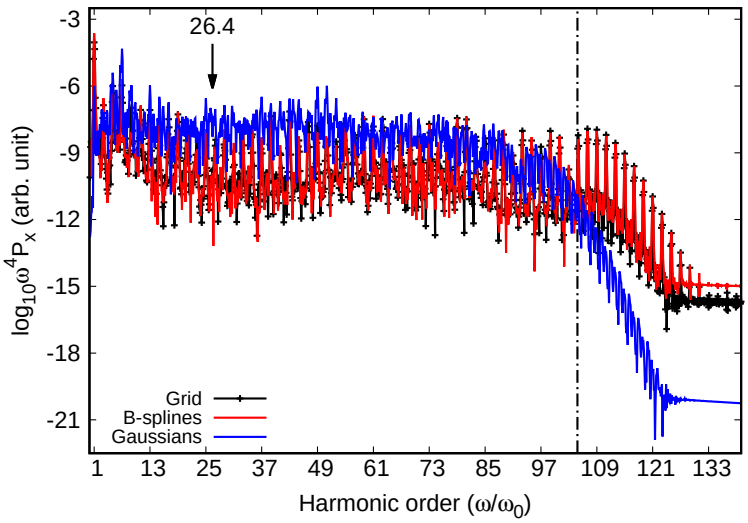

FIG. S5: HHG from the dipole at R = 2.0 au with laser intensity I=7×10^{14} W/cm^2. The dot-dashed line indicates the energy cutoff $E_{\text{cutoff}} = 104.9\omega_0$. The arrow points the expected position of the two center interference minimum extracted from the recombination dipole.

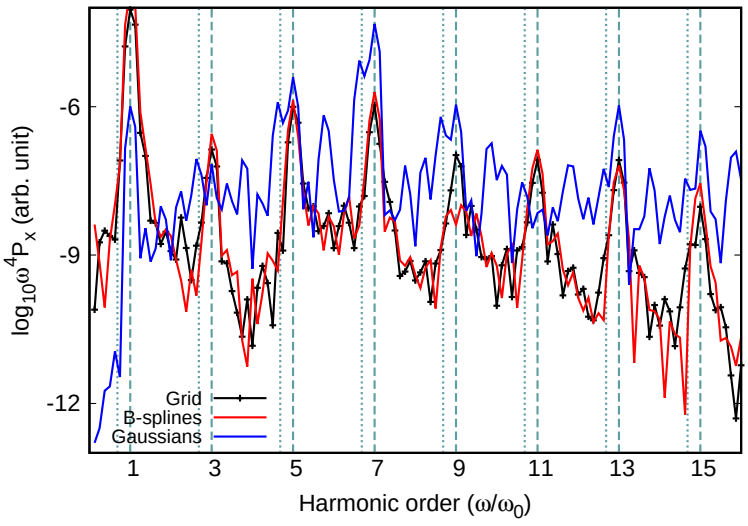

FIG. S6: HHG spectrum from the dipole form at $R = 2.0$ au with laser intensity $I = 7 \times 10^{14}$ W/cm^2 up to the 15th harmonic. The dashed line indicates the position of each harmonics while the dotted line indicates the resonances due to the first excited state of H_2^+.

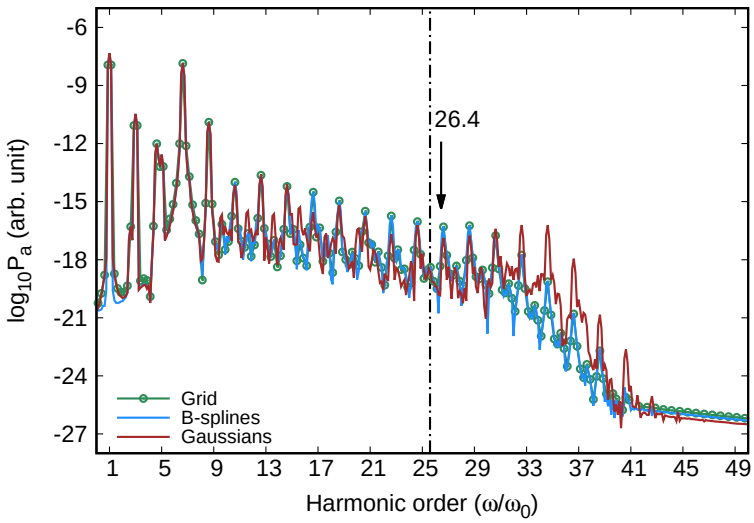

FIG. S7: HHG spectrum from the acceleration at $R = 2.0$ au with laser intensity $I = 5 \times 10^{13}$ W/cm^2. The dot-dashed line indicates the energy cutoff $E_{\text{cutoff}} = 25.6\omega_0$. The arrow points the expected position of the two-center interference minimum extracted from the recombination dipole.

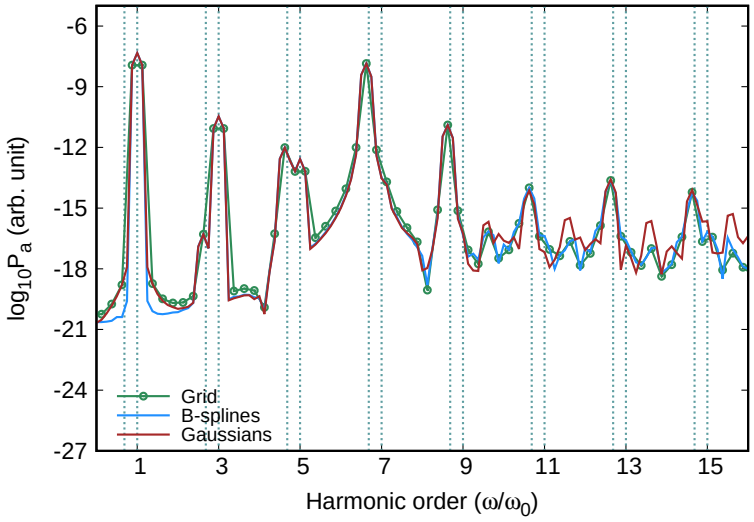

FIG. S8: HHG spectrum from the acceleration at $R = 2.0$ au with laser intensity $I = 5 \times 10^{13}$ W/cm^2 up to the 15th harmonic. The dashed line indicates the position of each harmonics while the dotted line indicates the resonances due to the first excited state of H_2^+.

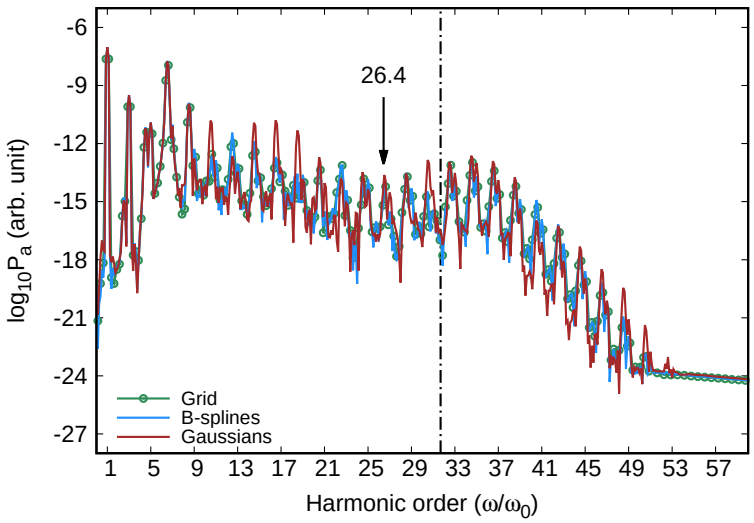

FIG. S9: HHG spectrum from the acceleration at $R = 2.0$ au with laser intensity $I = 1 \times 10^{14}$ W/cm^2. The dot-dashed line indicates the energy cutoff $E_{\text{cutoff}} = 31.7\omega_0$. The arrow points the expected position of the two-center interference minimum extracted from the recombination dipole.

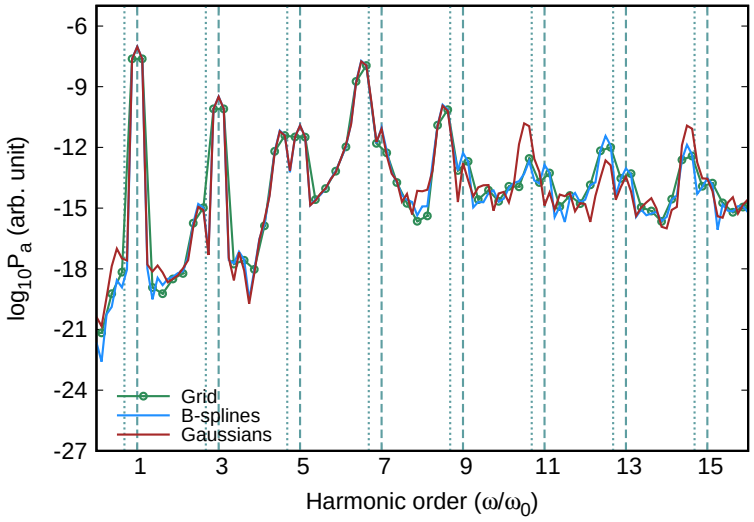

FIG. S10: HHG spectrum from the acceleration at $R = 2.0$ au with laser intensity $I = 1 \times 10^{14}$ W/cm^2 up to the 15th harmonic. The dashed line indicates the position of each harmonics while the dotted line indicates the resonances due to the first excited state of H_2^+.

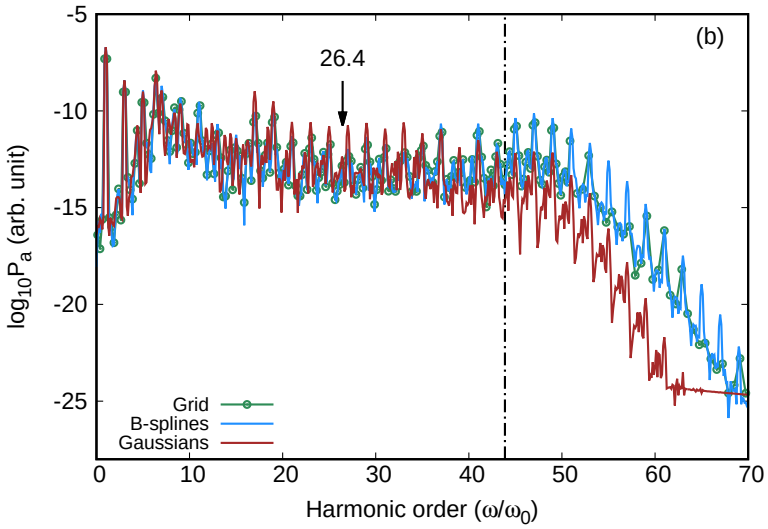

FIG. S11: HHG spectrum from the acceleration at $R = 2.0$ au with laser intensity $I = 2 \times 10^{14}$ W/cm^2. The dot-dashed line indicates the energy cutoff $E_{\text{cutoff}} = 43.9\omega_0$. The arrow points the expected position of the two-center interference minimum extracted from the recombination dipole.

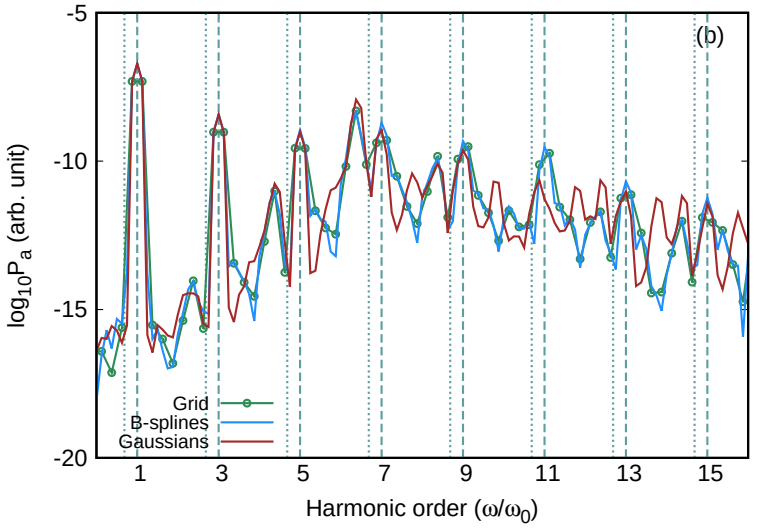

FIG. S12: HHG spectrum from the acceleration at $R = 2.0$ au with laser intensity $I = 2 \times 10^{14}$ W/cm^2 up to the 15th harmonic. The dashed line indicates the position of each harmonics while the dotted line indicates the resonances due to the first excited state of H_2^+.

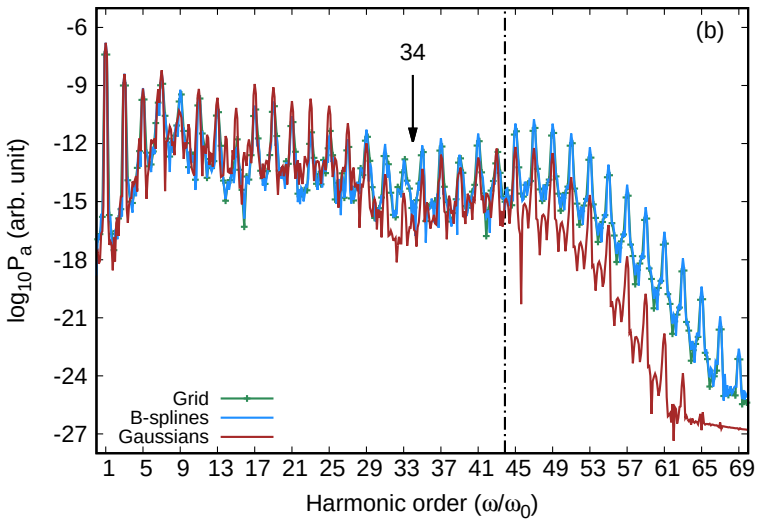

FIG. S13: HHG spectrum from the acceleration at $R = 1.8$ au with laser intensity $I = 2 \times 10^{14}$ W/cm^2. The dot-dashed line indicates the energy cutoff $E_{\text{cutoff}} = 43.9\omega_0$. The arrow points the expected position of the two-center interference minimum extracted from the recombination dipole.

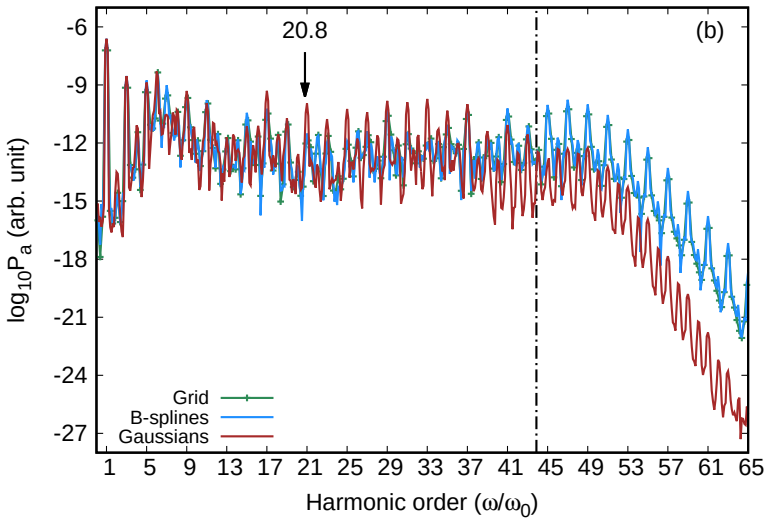

FIG. S14: HHG spectrum from the acceleration at $R = 2.2$ au with laser intensity $I = 2 \times 10^{14}$ W/cm^2. The dot-dashed line indicates the energy cutoff $E_{\text{cutoff}} = 43.9\omega_0$. The arrow points the expected position of the two-center interference minimum extracted from the recombination dipole.

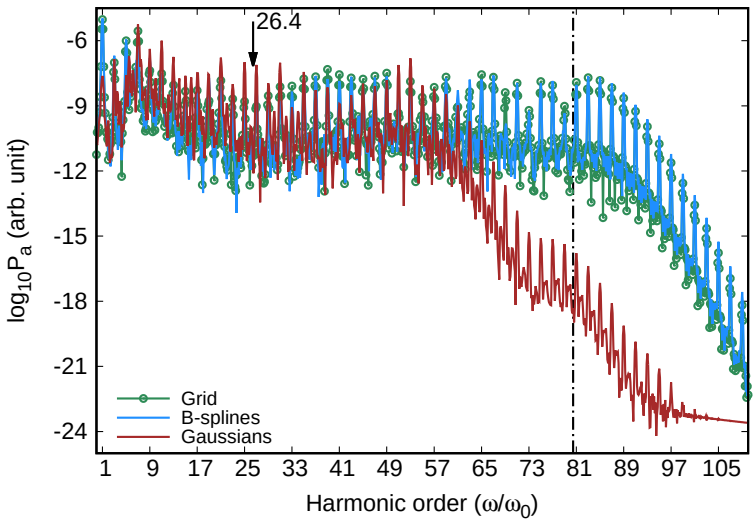

FIG. S15: HHG from the acceleration at R = 2.0 au with laser intensity I=5×10^{14} W/cm^2. The dot-dashed line indicates the energy cutoff $E_{\text{cutoff}} = 80.5\omega_0$. The arrow points the expected position of the two center interference minimum extracted from the recombination dipole.

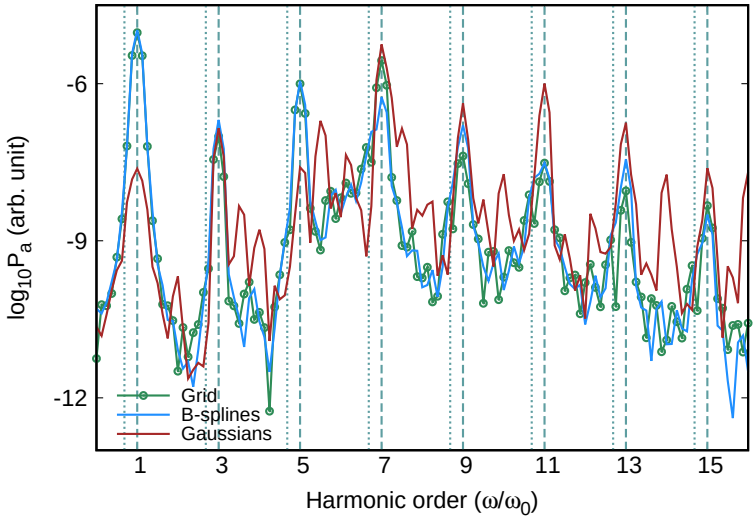

FIG. S16: HHG spectrum the acceleration at $R = 2.0$ au with laser intensity $I = 5 \times 10^{14}$ W/cm^2 up to the 15th harmonic. The dashed line indicates the position of each harmonics while the dotted line indicates the resonances due to the first excited state of H_2^+.

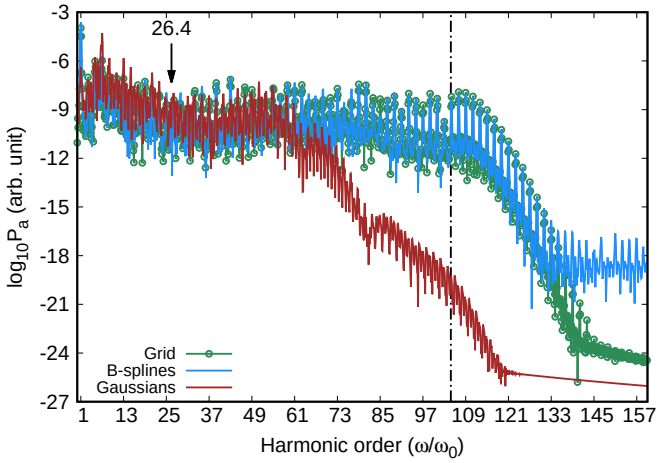

FIG. S17: HHG spectrum the acceleration at $R = 2.0$ au with laser intensity $I = 7 \times 10^{14}$ W/cm^2. The dot-dashed line indicates the energy cutoff $E_{\text{cutoff}} = 104.9\omega_0$. The arrow points the expected position of the two-center interference minimum extracted from the recombination dipole.

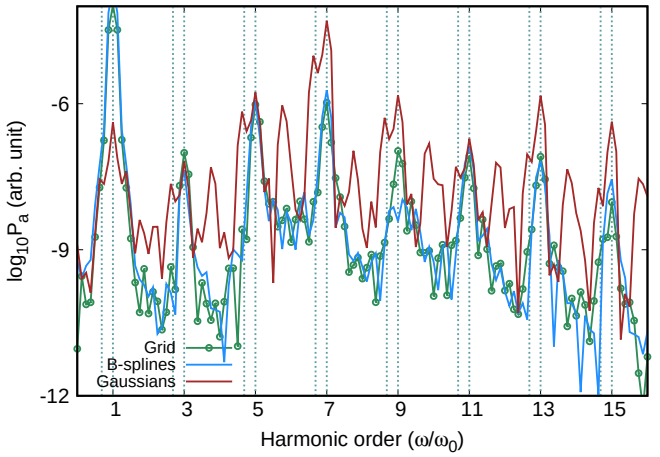

FIG. S18: HHG spectrum the acceleration at $R = 2.0$ au with laser intensity $I = 7 \times 10^{14}$ W/cm^2 up to the 15th harmonic. The dashed line indicates the position of each harmonics while the dotted line indicates the resonances due to the first excited state of H_2^+.

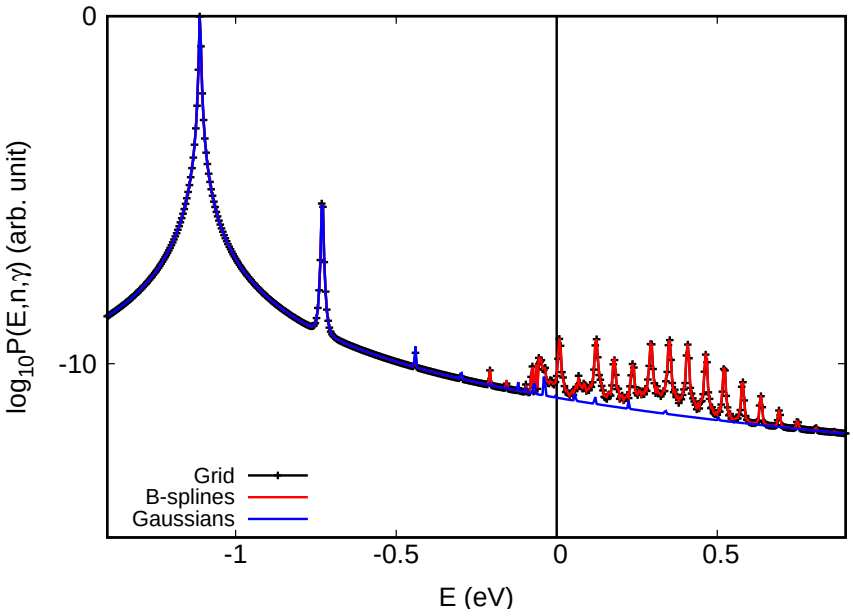

FIG. S19: ATI spectrum calculated at the equilibrium interatomic distance $R = 2.0$ au with laser intensity $I = 5 \times 10^{13}$ W/cm^2.

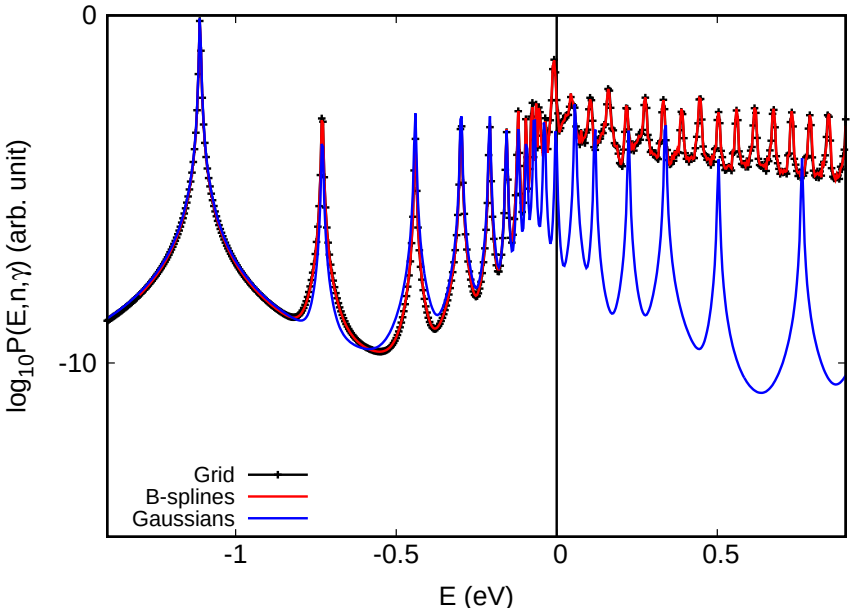

FIG. S20: ATI spectrum calculated at the equilibrium interatomic distance $R = 2.0$ au with laser intensity $I = 5 \times 10^{14}$ W/cm^2.

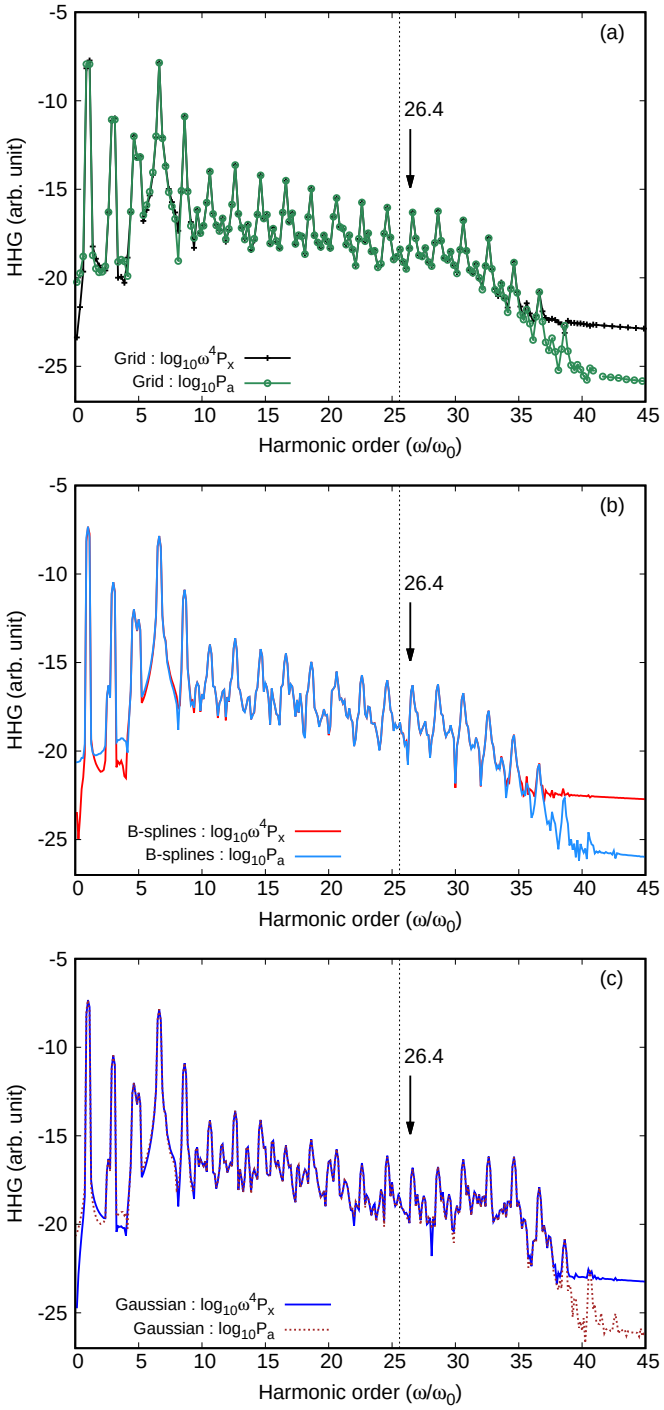

FIG. S21: HHG spectra from the dipole and the acceleration at the equilibrium internuclear distance of $R = 2.0$ au with laser intensity $I = 5 \times 10^{13}$ W/cm^2 calculated using the (a) grid, (b) B-spline, and (c) Gaussian basis sets. The dot dashed line is the cutoff energy $E_{\rm cutoff} = 25.6\omega_0$. The arrow points the expected position of the two-center interference minimum extracted from the recombination dipole.

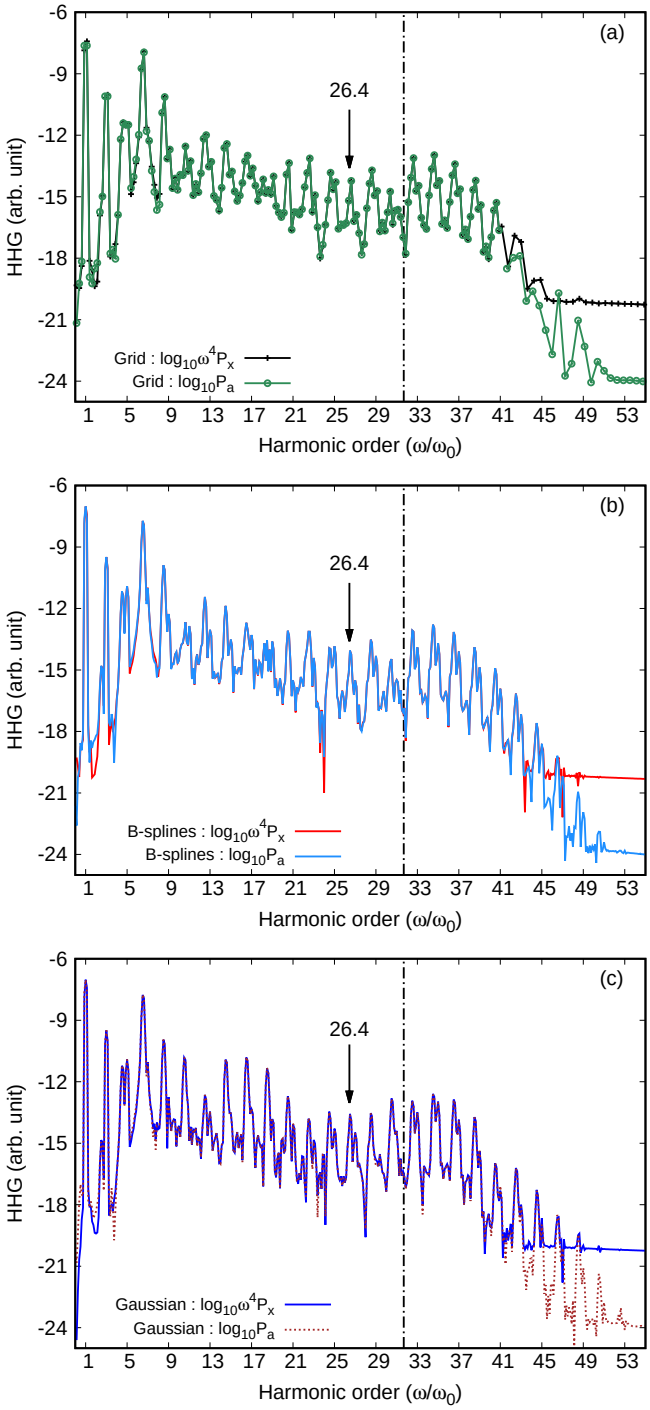

FIG. S22: HHG spectra from the dipole and acceleration at the equilibrium internuclear distance of $R = 2.0$ au with laser intensity $I = 1 \times 10^{14}$ W/cm^2 calculated using the (a) grid, (b) B-spline, and (c) Gaussian basis sets. The dot dashed line is the cutoff energy $E_{\text{cutoff}} = 31.7\omega_0$. The arrow points the expected position of the two-center interference minimum extracted from the recombination dipole.

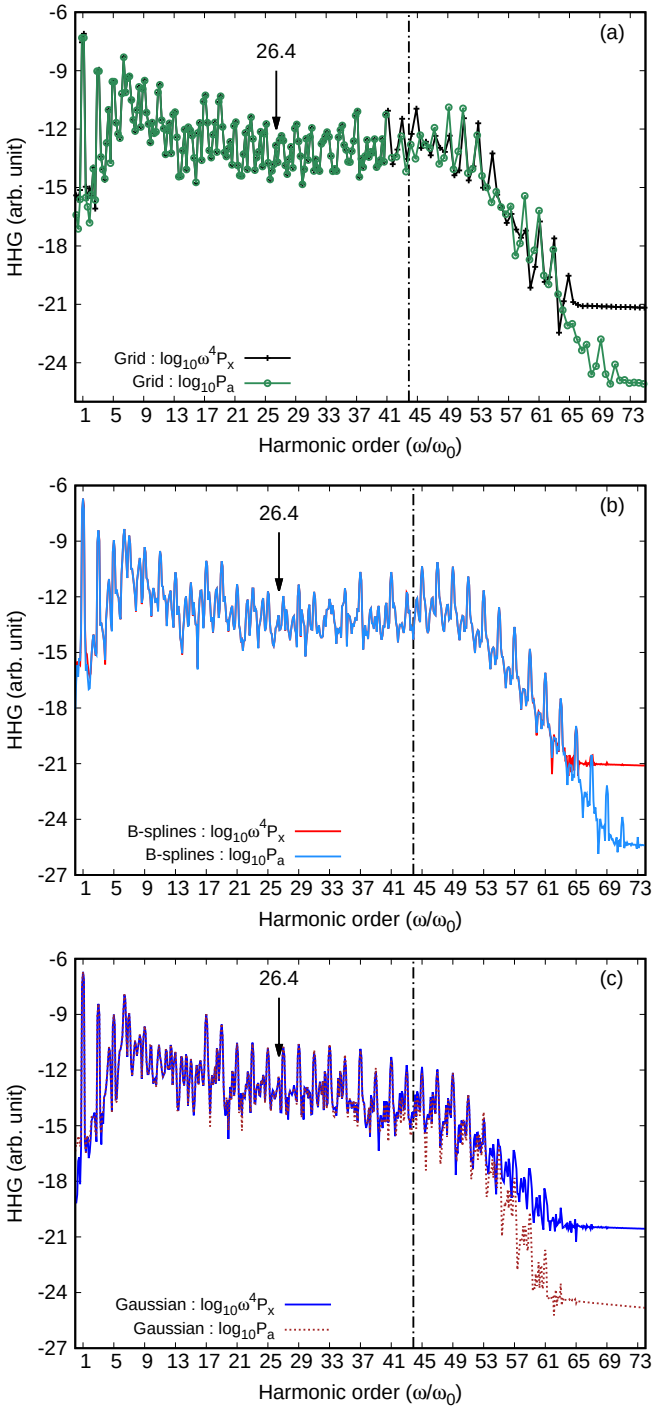

FIG. S23: HHG spectra from the dipole and the acceleration at the equilibrium internuclear distance of $R = 2.0$ au with laser intensity $I = 2 \times 10^{14}$ W/cm^2 calculated using the (a) grid, (b) B-spline, and (c) Gaussian basis sets. The dot dashed line is the cutoff energy $E_{\rm cutoff} = 43.9\omega_0$. The arrow points the expected position of the two-center interference minimum extracted from the recombination dipole.

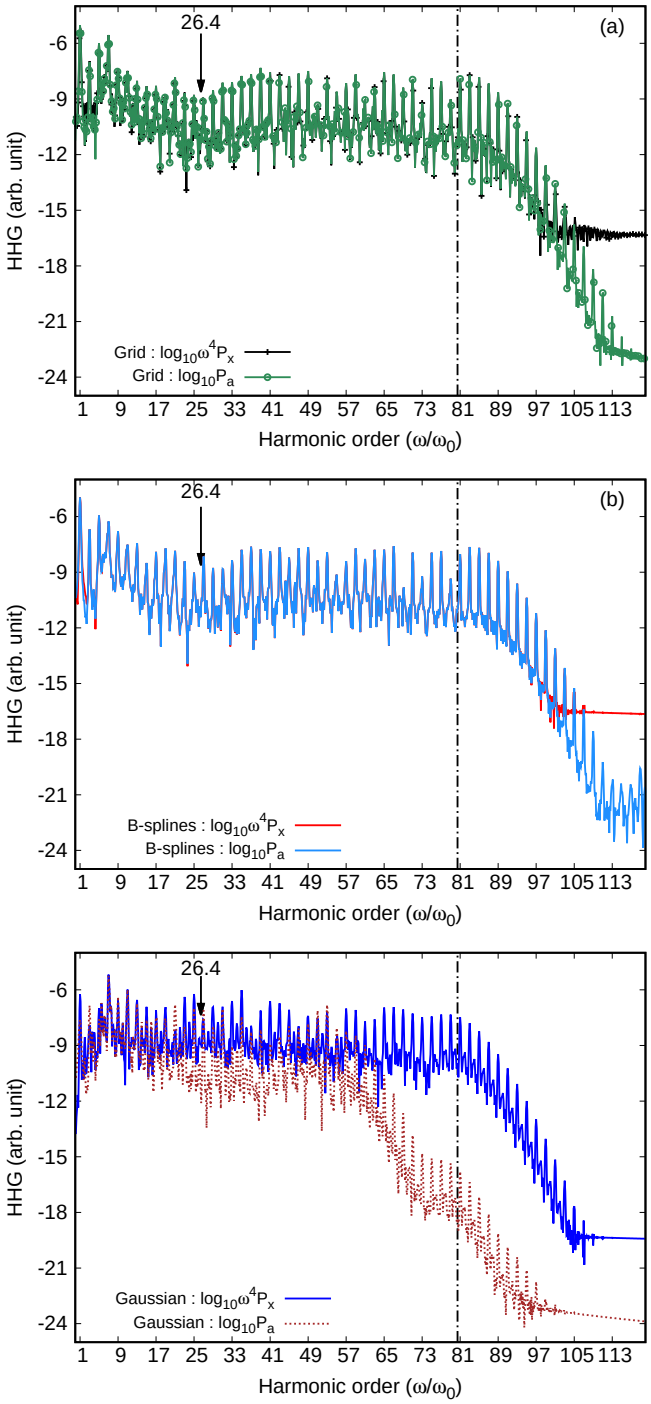

FIG. S24: HHG spectra from the dipole and the acceleration at the equilibrium internuclear distance of $R = 2.0$ au with laser intensity $I = 5 \times 10^{14}$ W/cm^2 calculated using the (a) grid, (b) B-spline, and (c) Gaussian basis sets. The dot dashed line is the cutoff energy $E_{\rm cutoff} = 80.5\omega_0$. The arrow points the expected position of the two-center interference minimum extracted from the recombination dipole.

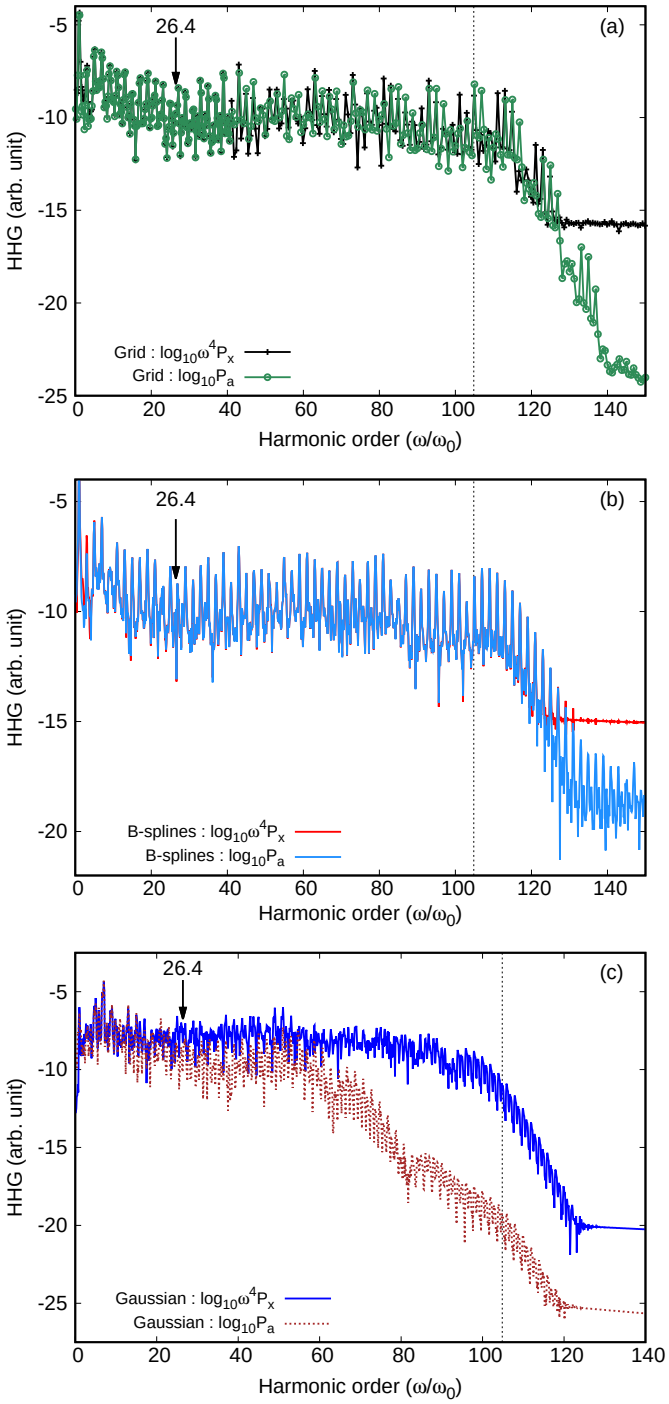

FIG. S25: HHG spectra from the dipole and the acceleration at the equilibrium internuclear distance of $R = 2.0$ au with laser intensity $I = 7 \times 10^{14}$ W/cm^2 calculated using the (a) grid, (b) B-spline, and (c) Gaussian basis sets. The dot dashed line is the cutoff energy $E_{\rm cutoff} = 104.9\omega_0$. The arrow points the expected position of the two-center interference minimum extracted from the recombination dipole.

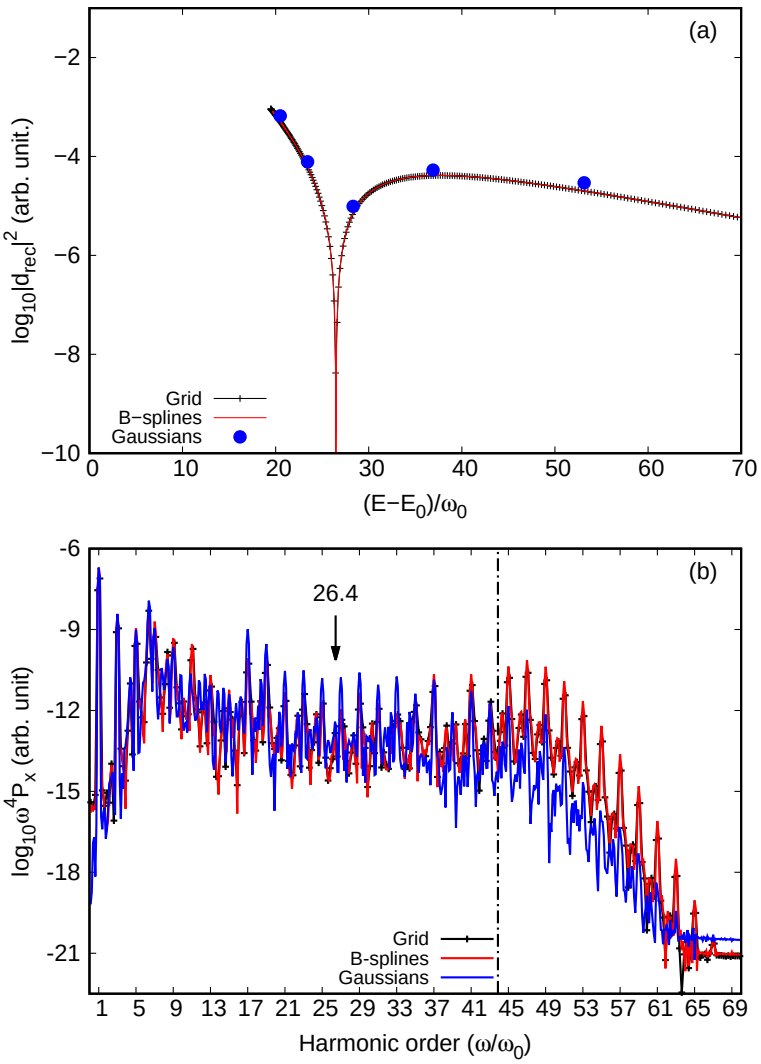

FIG. S26: Two center interferences at R = 2.0 au : (a) recombination dipole and (b) HHG from dipole at I=2×10^{14} W/cm^2. The arrow points to the expected position of the two center interference minimum extracted from the recombination dipole. The dot dashed line is the cutoff energy $E_{\text{cutoff}} = 43.9\omega_0$.

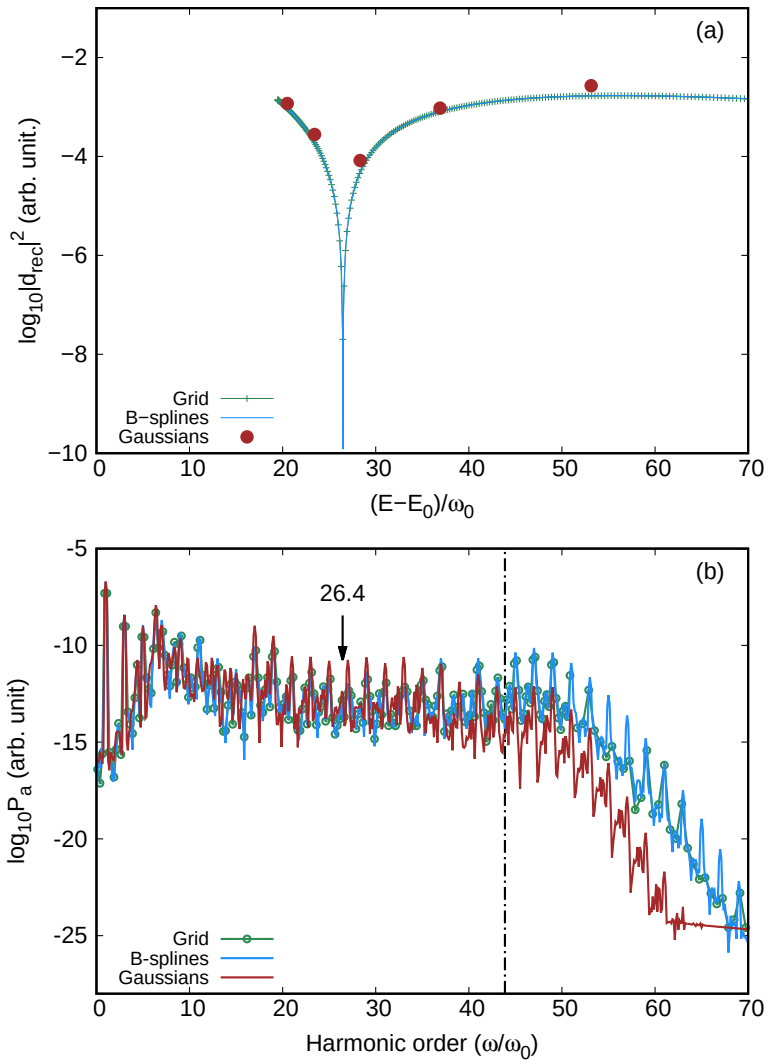

FIG. S27: Two-center interferences at $R = 2.0$ au: (a) recombination acceleration and (b) HHG spectrum acceleration at $I = 2 \times 10^{14}$ W/cm^2. The arrow points to the expected position of the two-center interference minimum extracted from the recombination acceleration. The dot dashed line is the cutoff energy $E_{\text{cutoff}} = 43.8\omega_0$.

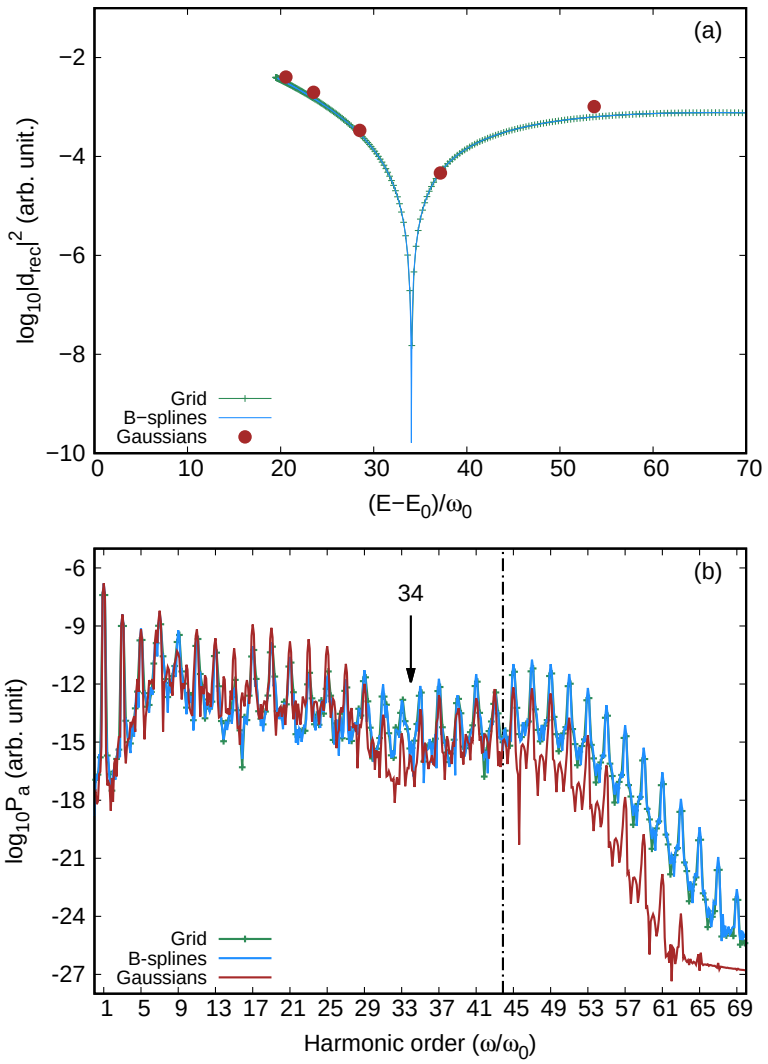

FIG. S28: Two-center interferences at $R = 1.8$ au: (a) recombination acceleration and (b) HHG spectrum acceleration at $I = 2 \times 10^{14}$ W/cm^2. The arrow points to the expected position of the two-center interference minimum extracted from the recombination acceleration. The dot dashed line is the cutoff energy $E_{\text{cutoff}} = 43.8\omega_0$.

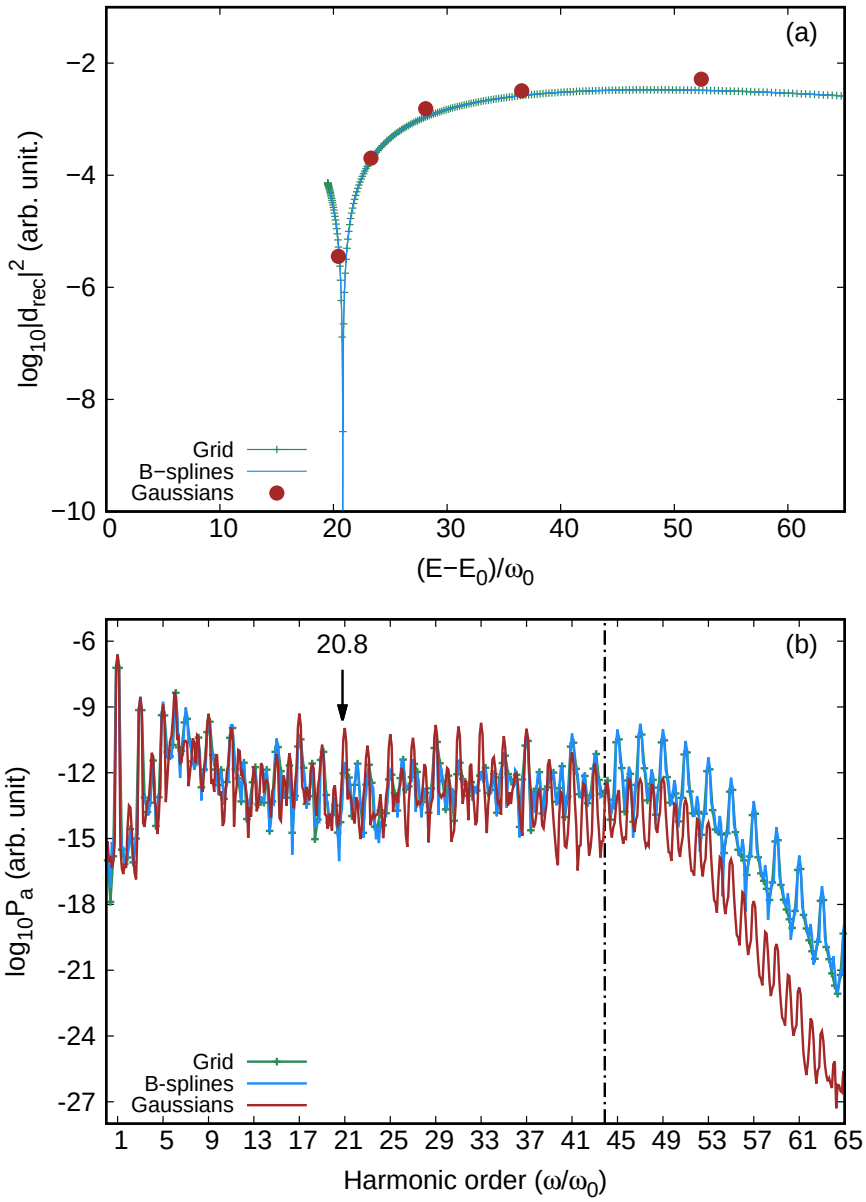

FIG. S29: Two-center interferences at $R = 2.2$ au: (a) recombination acceleration and (b) HHG spectrum acceleration at $I = 2 \times 10^{14}$ W/cm^2. The arrow points to the expected position of the two-center interference minimum extracted from the recombination acceleration. The dot dashed line is the cutoff energy $E_{\text{cutoff}} = 43.8\omega_0$.

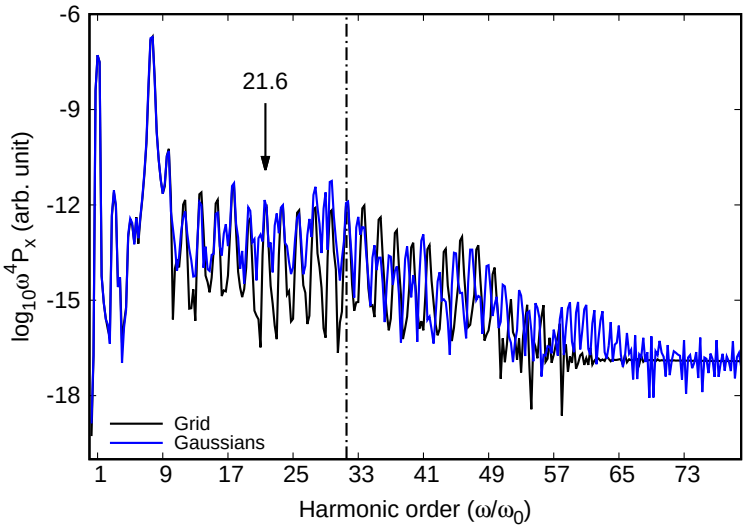

FIG. S30: HHG spectra calculated at the equilibrium interatomic distance $R = 2.0$ au with laser intensity $I = 1 \times 10^{14}$ W/cm^2. The dot dashed line is the cutoff energy $E_{\text{cutoff}} = 31.5\omega_0$.

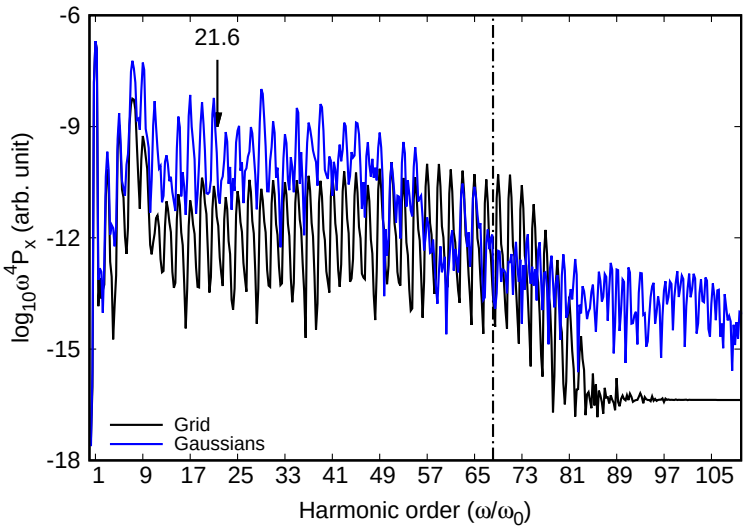

FIG. S31: HHG spectra calculated at the equilibrium interatomic distance $R = 2.0$ au with laser intensity $I = 4 \cdot 10^{14}$ W/cm^2. The dot dashed line is the cutoff energy $E_{\text{cutoff}} = 68.1\omega_0$.

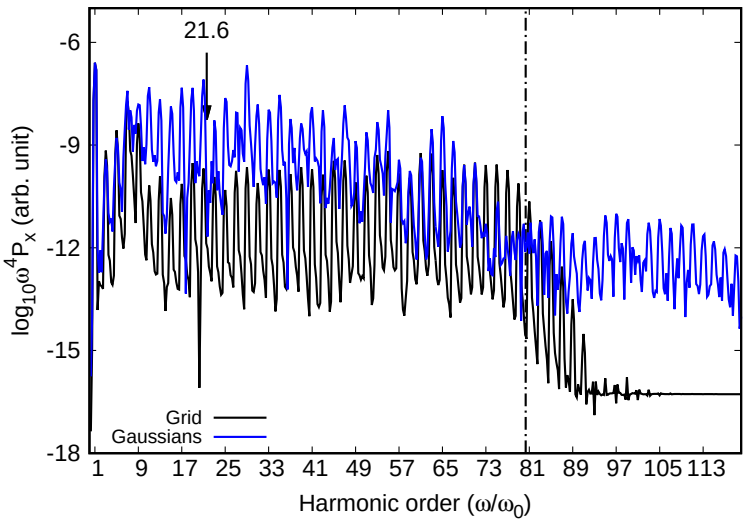

FIG. S32: HHG spectra calculated at the equilibrium interatomic distance $R = 2.0$ au with laser intensity $I = 5 \cdot 10^{14}$ W/cm^2. The dot dashed line is the cutoff energy $E_{\text{cutoff}} = 80.3\omega_0$.

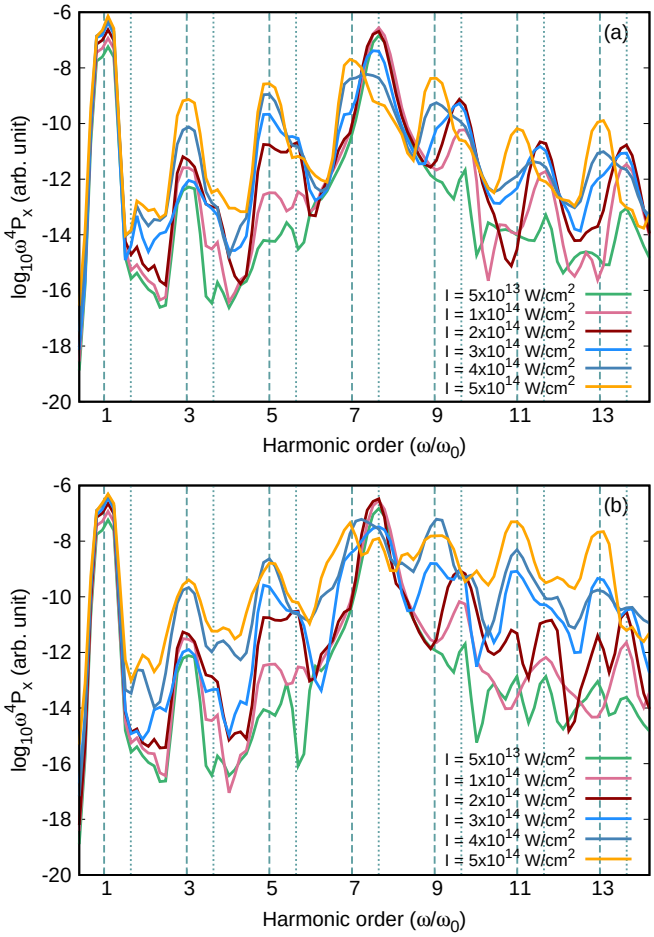

FIG. S33: HHG spectra in the dipole form at the equilibrium internuclear distance of $R = 2.0$ au up to the 13th harmonic with laser intensities: $I = 5 \times 10^{13}$ W/cm^2, $I = 1 \times 10^{14}$ W/cm^2, $I = 2 \times 10^{14}$ W/cm^2, $I = 3 \times 10^{14}$ W/cm^2, $I = 4 \times 10^{14}$ W/cm^2, and $I = 5 \times 10^{14}$ W/cm^2 for (a) grid and (b) Gaussian basis sets. For each HHG spectrum, the dashed line indicates the position of the harmonics and the dotted line indicates the resonances due to the first excited state of H_2^+.